

Charge and Orbital Order in Half-Doped Manganites

Jeroen van den Brink* and Giniyat Khaliullin†

Max-Planck-Institut für Festkörperforschung, Heisenbergstrasse 1, D-70569 Stuttgart, Germany

Daniel Khomskii

Laboratory of Applied and Solid State Physics, Materials Science Center, University of Groningen, Nijenborgh 4, 9747 AG Groningen, The Netherlands

(Received 2 August 1999)

An explanation is given for the charge order, orbital order, and insulating state observed in half-doped manganese oxides, such as $\text{Nd}_{1/2}\text{Sr}_{1/2}\text{MnO}_3$. The competition between the kinetic energy of the electrons and the magnetic exchange energy drives the formation of effectively one-dimensional ferromagnetic zigzag chains. Because of a topological phase factor in the hopping, the chains are intrinsically insulating and orbital ordered. Most surprisingly, the strong Coulomb interaction between electrons on the same Mn ion leads to the experimentally observed charge ordering. For doping less than $1/2$ the system is unstable towards phase separation into a ferromagnetic metallic and charge-ordered insulating phase.

PACS numbers: 75.30.Vn, 71.10.-w, 71.27.+a, 75.30.Et

Manganese oxides with the general composition $\text{R}_{1-x}\text{A}_x\text{MnO}_3$ (where R and A are rare- and alkaline-earth ions, respectively) have attracted considerable attention because of their unusual magnetic and electronic properties. In some of these materials, metal-insulator transitions can be observed where both conductivity and magnetization change markedly. The $x = 0$ and $x = 1$ end members of the $\text{R}_{1-x}\text{A}_x\text{MnO}_3$ family are insulating and antiferromagnetic (AF) with the Mn ion in the Mn^{3+} and Mn^{4+} state, respectively. For intermediate x , the average Mn valence is noninteger and the material is generally metallic or semiconducting. Most of the perovskite manganites show a ferromagnetic (FM) ground state when the holes are optimally doped (usually $0.2 < x < 0.5$) and anisotropic antiferromagnetic (AFM) phases for $x > 0.5$. The half-doped manganites, with $x = \frac{1}{2}$, are very particular. Magnetically these systems form FM zigzag chains that are coupled AFM (see Fig. 1) at low temperatures, the so-called magnetic CE phase [1]. The ground state is, moreover, an orbital-ordered and charge-ordered insulator. This behavior is generic and is experimentally observed in $\text{Nd}_{1/2}\text{Sr}_{1/2}\text{MnO}_3$ [2,3], $\text{Pr}_{1/2}\text{Sr}_{1/2}\text{MnO}_3$ [4], $\text{Pr}_{1/2}\text{Ca}_{1/2}\text{MnO}_3$ [5], $\text{La}_{1/2}\text{Ca}_{1/2}\text{MnO}_3$ [6,7], $\text{Nd}_{1/2}\text{Ca}_{1/2}\text{MnO}_3$ [8], and in the half-doped layered manganite $\text{La}_{1/2}\text{Sr}_{3/2}\text{MnO}_4$ [9]. The insulating charge-ordered state can be transformed into a metallic FM state by application of an external magnetic field, a transition that is accompanied by a change in resistivity of several orders of magnitude [2,10].

The occurrence of charge order, orbital order, and large magnetoresistance in the half-doped manganites is experimentally well established. Theoretically, however, the nature of the charge ordering at $x = \frac{1}{2}$ and the origin of the unconventional zigzag magnetic structure remain unclear. We address these points here and show that (i) the insulating CE phase results from a particular

ordering of orbitals, (ii) this state is stable only in a narrow concentration range around the commensurate value, and (iii) the zigzag chains are intrinsically charge ordered due to on-site Hubbard correlations.

The competition between kinetic energy (double-exchange) and superexchange between the manganese core spins, combined with the orbital degeneracy leads to the formation of the magnetic CE phase, for the same reasons as it leads to the anisotropic magnetic phases in the highly doped manganites with $x > \frac{1}{2}$ [11]. The CE phase is found to be stable close to $x = \frac{1}{2}$; for $x > 0.57$ the C phase is stable and for $x < \frac{1}{2}$ we find phase separation between the CE phase and FM phase.

As in the double-exchange framework, electrons can only hop between sites with FM aligned core spins, in the CE phase only hopping processes within the zigzag chains are possible, rendering the system one dimensional for low-energy charge fluctuations. The essential observation is that an electron that passes a corner site of the zigzag

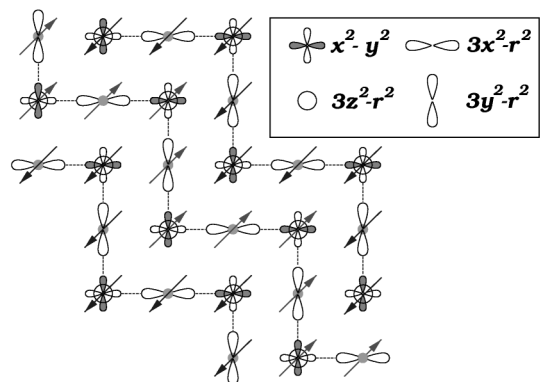


FIG. 1. View of the CE phase in the x - y plane. We choose our basis orbitals such that the gray lobes of the shown orbitals have a negative sign. The dots at the bridge sites represent a charge surplus.

chain, acquires a phase that depends on the orbital through which it passes. This leads to an effective dimerization that splits the bands and opens a gap at the Fermi surface. The gap is very robust as it is a consequence of the staggered phase factor that is itself fully determined by the topology of the system. At the same time not all orbitals are fully occupied, leading to an orbital-polarized ground state. Our most surprising observation is that the experimentally observed charge order is directly obtained from the degenerate double-exchange model when the Coulomb interaction (the Hubbard U) between electrons in different orbitals, but *on the same site* is included. This can be understood from the fact that in the band picture on the corner sites both orthogonal orbitals are partially occupied, but on the bridge site only one orbital is partially filled. The on-site Coulomb interaction acts therefore differently on the corner and bridge sites: charge is pushed away from the effectively correlated corner sites to the effectively uncorrelated bridge sites.

The theoretical explanation for the ferromagnetic metallic state in doped manganites was already developed in the 1950s and 1960s [12–14]. The number of d electrons per manganese site is $4 - x$. Three electrons occupy the low-lying t_{2g} orbitals, having parallel spins. The other electrons occupy the e_g orbitals with their spin parallel to the t_{2g} spin because of the large ferromagnetic Hund's rule exchange J_H . In the double-exchange framework electrons can only hop from one Mn site to a neighboring one, when the t_{2g} spins of these sites are aligned ferromagnetically because otherwise, in the classical treatment of the t_{2g} core-spin the electron would have to overcome an energy barrier proportional to J_H .

On the other hand, the conventional superexchange favors AF alignment of the spins. This leads to an intricate competition between the kinetic energy and the superexchange [14] that is amplified by the twofold degeneracy of the e_g levels in a cubic crystal. As a basis for the e_g wave functions we take the $x^2 - y^2$ ($|\chi\rangle$) and $3z^2 - r^2$ ($|\zeta\rangle$) orbitals. The hopping of the electrons between neighboring Mn sites depends strongly on the kind of the orbitals involved and on the direction of the bond. The Hamiltonian for the kinetic energy is

$$H_t = t \sum_{\alpha,\beta,\langle ij \rangle_\Gamma} M_{\alpha,\beta}^\Gamma c_{i,\alpha}^+ c_{j,\beta}, \quad (1)$$

where $c_{i,\alpha}^+$ creates an electron on site i in orbital α and $\langle ij \rangle_\Gamma$ denotes a nearest-neighbor pair along the Γ direction ($\Gamma = x, y, z$) and t is the hopping integral. The hopping is constrained to nearest-neighbor Mn ions that have FM aligned t_{2g} core spins (canted phases are not important in the doping range we consider here.) The matrices $M_{\alpha,\beta}^x$ and $M_{\alpha,\beta}^y$ can be found by applying the cubic symmetry operations on $M_{\alpha,\beta}^z$, where $M_{|\zeta\rangle,|\zeta\rangle}^z = 1$ and all other matrix elements are zero. This means physically that along the z direction, for instance, electrons can only hop between $|\zeta\rangle$ orbitals and that all other hoppings (involving at least one $|\chi\rangle$ orbital) are zero by symmetry, whereas in the x and y direction all hoppings are allowed

(and related by symmetry). The strong spatial anisotropy of the hopping, combined with the competing kinetic and superexchange energy J can, depending on the e_g bandwidth and J , give rise to low dimensional spin-structures that, for instance, optimize kinetic energy by forming FM chains and optimize magnetic energy by a AFM coupling of these chains (C phase), or AFM coupled FM planes (A phase) [11].

In the homogenous FM state at $x = \frac{1}{2}$ the magnetic energy per site is $E_{\text{mag}}^{\text{FM}} = 3J$ and the kinetic energy per site $E_{\text{kin}}^{\text{FM}} = -t$, if the t_{2g} spin is treated as a classical spin. Here the magnetic energy is found by determining the number of AFM bonds, and the kinetic energy from the filling of the bands, as is described in Ref. [11]. For AFM coupled FM chains, the C phase, $E_{\text{kin}}^C + E_{\text{mag}}^C = -0.6366t + J$, so that the C phase is stable with respect to the FM phase for $J > 0.1816t$. A third possibility is for the spins to form FM zigzag chains that are coupled AFM, the CE phase [1]; see Fig. 1. The CE phase is always higher in energy than the C phase, except close to $x = \frac{1}{2}$. For the half-doped system $E_{\text{kin}}^{\text{CE}} + E_{\text{mag}}^{\text{CE}} = -0.695t + J$. It is easily shown that the A phase is higher in energy. Thus for the half-doped manganites the experimentally observed CE phase is indeed lower in energy than the C phase, and lower than the FM phase when $J > 0.1524t$.

Let us address our main findings that the CE phase is charge ordered, orbital ordered, and insulating, and come back to the stability of the CE phase at the end of the paper. As shown in Fig. 1 the CE phase contains two geometrically inequivalent sites, so-called bridge and corner sites. Note that our specific choice of basis orbitals as shown in Fig. 1 is motivated by the convenience of this basis for the calculations. The expectation value of actual observables is, of course, independent from the choice of basis Wannier orbitals. The topology of the electron hopping integrals is shown in Fig. 2. The crucial

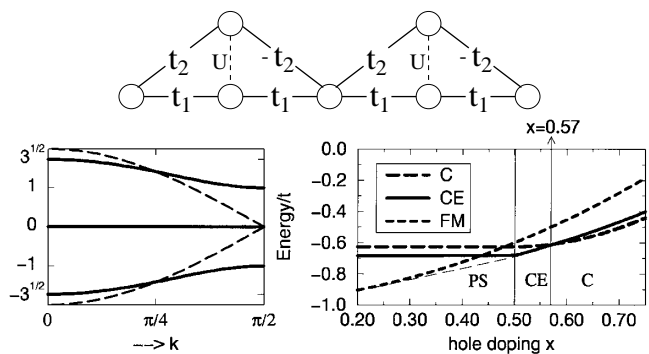


FIG. 2. Top: Topology of the interactions in a zigzag chain, where $t_1 = t/2$, $t_2 = t\sqrt{3}/2$, and U is the Coulomb interaction between electrons on the same site. Bottom left: electron dispersion in the zigzag chain of the CE phase for $U = 0$ and electron dispersion in a straight chain, as in C phase (dashed line). Bottom right: total energy per site for the CE, C , and FM phase for $t/J = 5$. The Maxwell construction in the phase separated (PS) region is shown by the thin dashed line.

observation is that an electron that hops from one bridge site to another bridge site via a $|\chi\rangle$ corner orbital obtains a phase factor -1 , while if the hopping takes place via a $|\zeta\rangle$ corner orbital, the phase factor is $+1$.

The bands are obtained by the solution of a 3×3 matrix. There are two bands with energy $\epsilon_{\pm} = \pm t\sqrt{2 + \cos k}$, where k is the wave vector, and two nondispersive bands at zero energy; see Fig. 2 [15]. At $x = \frac{1}{2}$ the ϵ_- band is fully occupied, and all other bands are empty. The system is insulating as the occupied and empty bands are split by a gap $\Delta = t$. In the C and CE phase the magnetic energies are equal, but the opening of the gap at the Fermi energy in the CE phase lowers its energy if the bands are half filled. This mechanism is equivalent to the situation in the lattice-Peierls problem, where the opening of a gap stabilizes a ground state with a lattice deformation.

In the insulating state the average occupancy of the bridge site $3x^2 - r^2$ ($3y^2 - r^2$) orbital is $\frac{1}{2}$, while the orthogonal bridge orbital is empty. The average occupancy of the corner site is also $\frac{1}{2}$, with the ratio between $|\chi\rangle$ and $|\zeta\rangle$ occupancy of $\sqrt{3}:1$. The system is therefore orbital ordered, but charge is homogeneously distributed between corner and bridge sites.

This changes drastically when also the Coulomb interaction U between electrons on the same site is taken into account. The Hamiltonian is

$$H_U = U \sum_{\alpha < \beta, i} n_{i,\alpha} n_{i,\beta}, \quad (2)$$

where $n_{i,\alpha} = c_{i,\alpha}^\dagger c_{i,\alpha}$. For the e_g electrons in the manganites $U \approx 10t$, so that the system is strongly correlated. The correlations, however, have a very different effect on the corner and bridge sites. On the bridge site, one orbital is always empty, so that the Coulomb repulsion is ineffective, whereas on the corner sites both orbitals are partially occupied. The consequence is that charge is pushed away from the correlated corner sites to the effectively uncorrelated bridge sites, causing charge order.

We treat the full Hamiltonian $H = H_t + H_U$ for $x = \frac{1}{2}$ with three different methods: exact diagonalization (ED), in mean field (MF) and with the Gutzwiller projection (GP) [16]. In the ED calculation we consider a ring of 12 and 14 sites (or 18 and 21 orbitals, respectively) with the topology as in Fig. 2. In Fig. 3 the charge-disproportionation δ as a function of U/t is shown, where δ is defined as $\langle n_B - n_A \rangle$, where $\langle n_B \rangle$ ($\langle n_A \rangle$) is the expectation value for finding an electron on a bridge (corner) site. The results for the 12-site and 14-site cluster differ by less than 2% and finite size effects are therefore very small. For $U/t = 0$ also $\delta = 0$, as explained above, and for finite Coulomb interaction δ monotonously increases with U . For $U/t = 10$, $\delta = 0.171$ and δ reaches its maximum value for $U \rightarrow \infty$. In a ED calculation for a 16-site cluster with $U \rightarrow \infty$, we find that $\delta_{\infty}^{\text{ED}} = 0.185$.

For small values of U/t a MF treatment is expected to be very reliable because the charge fluctuations are gapped. We decouple the quartic term in Eq. (2)

and determine the charge densities in the orbitals self-consistently. The results for small U/t are shown with a dashed line in Fig. 3 and they agree very well with the ED results for $U < \Delta$. In the GP, valid for $U \rightarrow \infty$, we introduce constrained electrons on the correlated corner site. For the $|\chi\rangle$ orbital we introduce $\bar{x}_i = (1 - n_i^z)x_i$ and for the $|\zeta\rangle$ orbital $\bar{z}_i = (1 - n_i^x)z_i$, where x_i (z_i) denotes an electron operator on corner site i , with corresponding density n_i^x (n_i^z) and \bar{x}_i (\bar{z}_i) a constrained electron operator. The Hamiltonian is

$$H_{\text{GP}} = \sum_{i \in B} c_i^\dagger [t_1(\bar{z}_{i+1} + \bar{z}_{i-1}) + t_2(\bar{x}_{i+1} - \bar{x}_{i-1})] + \text{H.c.}, \quad (3)$$

which physically means that an electron can hop to a $|\chi\rangle$ orbital on a corner site only when there is no electron in the $|\zeta\rangle$ orbital on that site and *vice versa*, so that a corner site can never be occupied by more than one electron, as is required in the U -infinity limit. We decouple the quartic terms in H_{GP} as $c_{i+1}^\dagger z_i n_i^x \rightarrow c_{i+1}^\dagger z_i \langle n_i^x \rangle + \langle c_{i+1}^\dagger z_i \rangle n_i^x$. After a Fourier transform we find

$$H_{\text{GP}}^{\text{mf}} = \sum_k \epsilon_x x_k^\dagger x_k + \epsilon_z z_k^\dagger z_k + \tilde{t}_{1k}(c_k^\dagger z_k + z_k^\dagger c_k) + \tilde{t}_{2k}(c_k^\dagger x_k + x_k^\dagger c_k), \quad (4)$$

with $\epsilon_x = -4t_1 \sum_k \cos k \langle c_k^\dagger z_k \rangle$, $\epsilon_z = 4it_2 \sum_k \sin k \langle c_k^\dagger x_k \rangle$, $\tilde{t}_{1k} = 2t_1 \langle 1 - n^x \rangle \cos k$, and $\tilde{t}_{2k} = -2it_2 \langle 1 - n^z \rangle \sin k$. We obtain the solution of this system of equations by iteration, and find the charge-disproportionation $\delta_{\infty}^{\text{GP}} = 0.191$, which is represented by the dashed line in Fig. 3 for large U/t , and agrees well with the ED results.

The on-site Coulomb interaction causes a charge-surplus on the bridge sites in the x - y plane. In the CE structure the zigzag chains are stacked AFM along the z direction, which implies that above each bridge site there is another bridge site in the next plane. So we find that the charges actually accumulate on sheets formed by the bridge sites along the z direction. This is in remarkable

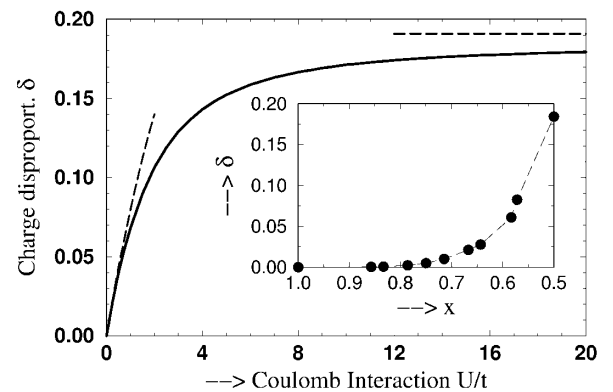


FIG. 3. Charge-disproportionation as a function of Coulomb interaction and doping (inset). The full line is obtained from exact diagonalization (ED) of a 14 site cluster. The dashed lines for small and large U are obtained by the mean-field and Gutzwiller approximations, respectively. The dots in the inset are the ED results for a 12 and 14 site cluster for $U \rightarrow \infty$.

agreement with experiment and at the same time excludes the possibility that the charge order is driven by longer range Coulomb interactions because the Madelung sum is always minimized for a rocksalt-type charge order. Similar physics may also apply to the situation at $x > 0.5$, e.g., for the stripe phases observed in Ref. [7].

Figure 3 shows that the charge disproportionation is strongly doping dependent. For $x > \frac{1}{2}$ the holes that are doped into the lower ϵ_- band efficiently suppress charge order. In this doping range, however, the CE phase becomes unstable with respect to the C phase. In Fig. 2 is shown that the kinetic energy of the C phase is lower for $x > 0.57$. For $x < \frac{1}{2}$ the energy per site of the CE phase, E_{CE} , is constant because the extra electrons are doped in the nondispersive bands at zero energy, which causes a kink of E_{CE} at $x = \frac{1}{2}$. For lower hole doping (higher electron concentration) the homogeneous FM phase is lower in energy, as is expected. The stability of the phases can be tested by performing a Maxwell construction. Because of the kink in E_{CE} at $x = \frac{1}{2}$, one finds that for $x < \frac{1}{2}$ the FM phase and CE phase coexist. The doping region where this phase separation occurs depends strongly on the actual value of the electron bandwidth and magnetic exchange. We conclude that there is a strong asymmetry for doping lower and higher than $\frac{1}{2}$, as phase separation between the CE and FM phases is present only on the lower doping side. Inclusion of the correlations beyond the mean-field approximation and longer range Coulomb interactions, which we did not consider in the calculation of total energies, may modify these results. On the basis of the ED results we believe, however, that U has only a small effect on the total energies. A more relevant contribution to the total energy comes from lattice deformations, as it is obvious that in the Jahn-Teller distorted C and, to a lesser extent, CE phases [17], there is a large gain in lattice energy with respect to the undistorted FM phase. It can be shown that the lattice contributions to the ground-state energy can, to a large extent, be described by using effective values of J [18], so that our general conclusions about phase separation for $x < \frac{1}{2}$ and about the asymmetry of the phase diagram for $x < \frac{1}{2}$ and $x > \frac{1}{2}$ remain valid. Recently this phase separation into a FM metallic and a charge ordered AFM insulating phase was observed experimentally [19].

In summary, we have given an explanation for the charge order, orbital order, and insulating state of the half-doped manganese oxides. The CE phase with one-dimensional ferromagnetic zigzag chains is stable for $x = \frac{1}{2}$ and due to staggered phase factors in the hopping,

the chains are insulating and orbital ordered. The striking feature of our model is that the strong Coulomb interaction between electrons on the same Mn site leads to the experimentally observed charge ordering. In a magnetic field, we expect the chains to be unstable with respect to the ferromagnetic metallic state. This might offer a likely explanation for the large magnetoresistance at the metal-insulator transition for the half-doped manganites.

We thank I. Solovyev and P. Horsch for useful discussions. J. v. d. B. acknowledges with appreciation the support by the Alexander von Humboldt-Stiftung, Germany. This work was financially supported by the Nederlandse Stichting voor Fundamenteel Onderzoek der Materie (FOM) and by the European network OXSEN.

*Present address: Department of Applied Physics, University of Twente, Enschede, The Netherlands.

†Permanent address: Kazan Physicotechnical Institute, 420029 Kazan, Russia.

- [1] E.O. Wohlen and W.C. Koehler, *Phys. Rev.* **100**, 545 (1955).
- [2] H. Kuwahara *et al.*, *Science* **270**, 961 (1995).
- [3] H. Kawano *et al.*, *Phys. Rev. Lett.* **78**, 4253 (1997).
- [4] Y. Tomioka *et al.*, *Phys. Rev. Lett.* **74**, 5108 (1995).
- [5] Z. Jirac *et al.*, *J. Magn. Magn. Mater.* **53**, 153 (1985); Y. Tomioka *et al.*, *Phys. Rev. B* **53**, R1689 (1996).
- [6] Y. Okimoto *et al.*, *Phys. Rev. Lett.* **75**, 109 (1995); P. Schiffer *et al.*, *ibid.* **75**, 3336 (1995); P.G. Radaelli *et al.*, *ibid.* **75**, 4488 (1995); Y. Okimoto *et al.*, *Phys. Rev. B* **55**, 4206 (1997).
- [7] S. Mori, C.H. Chen, and S.-W. Cheong, *Nature (London)* **392**, 473 (1998).
- [8] T. Kimura *et al.* (unpublished).
- [9] Y. Moritomo *et al.*, *Phys. Rev. B* **51**, 3297 (1995); B.J. Sternlieb *et al.*, *Phys. Rev. Lett.* **76**, 2169 (1996); Y. Moritomo *et al.*, *Nature (London)* **380**, 141 (1996).
- [10] M. Tokunaga *et al.*, *Phys. Rev. B* **57**, 5259 (1998).
- [11] J. van den Brink and D. Khomskii, *Phys. Rev. Lett.* **82**, 1016 (1999).
- [12] C. Zener, *Phys. Rev.* **82**, 403 (1951).
- [13] P.W. Anderson and H. Hasegawa, *Phys. Rev.* **100**, 675 (1955).
- [14] P.G. de Gennes, *Phys. Rev.* **118**, 141 (1960).
- [15] I.V. Solovyev and K. Terakura, *Phys. Rev. Lett.* **83**, 2825 (1999); T. Hotta *et al.* (unpublished).
- [16] See, for instance, P. Fulde, *Electron Correlations in Molecules and Solids* (Springer-Verlag, Berlin, 1991).
- [17] Note that the orbital polarization on the corner sites in the CE phase is not complete.
- [18] J. van den Brink and G. Khaliullin (unpublished).
- [19] N.A. Babushkina *et al.*, *Phys. Rev. B* **59**, 6994 (1999); M. Uehara *et al.*, *Nature (London)* **399**, 560 (1999).